# Coherent orientation relationship among various quasicrystalline and crystalline phases in rapidly solidified $Al_{78}Mn_{20}Ge_2$ alloy

N. P. Lalla, R. S. Tiwari, and O. N. Srivastava
*Physics Department, Banaras Hindu University, Varanasi - 221 005, India*

(Received 17 July 1991; accepted 23 August 1991)

Rapidly solidified $Al_{78}Mn_{20}Ge_2$ alloy exhibits a curious structural feature; this corresponds to the simultaneous occurrence of almost all the quasicrystalline phases, e.g., primitive and face-centered icosahedral phase, rational approximant, and a new metastable cubic phase. The cubic crystalline phase shows yet another type of recently observed twin relation which effectively produces an icosahedral symmetry, a feature that has so far been specific to alloy systems Al–Mn–Si and Al–Mn–Fe–Si only. The diffraction evidences obtained in the present investigation reveal that the orientation of the structural subunit, which is a MacKay icosahedron, remains invariant across the various interphase boundaries. These results elucidate clearly the structural interrelationship among the various phases.

## I. INTRODUCTION

Since the original discovery of an icosahedral quasicrystalline phase[1] in a rapidly solidified Al–Mn alloy, several other types of quasicrystalline and related phases have been found in different alloy systems.[2–9] Thus the family of quasicrystalline phases includes primitive and face-centered icosahedral, decagonal, rational approximants, and one-dimensional quasiperiodic structures. Out of the above-mentioned quasicrystalline phases, the face-centered icosahedral (FCI) quasicrystal has been discovered recently[7,10] and its occurrence is limited as far as we know to the alloy system in a specific compositional range in the alloys typified by $Al_{65}Cu_{20}M_{15}$ (M = Cr, Mn, Fe, Ru, and Os).[6] Thus, it is not yet understood whether the occurrence of the FCI type quasicrystal is more general or restricted to only certain alloy systems with specific compositional ranges. Furthermore, the various quasicrystalline phases, e.g., icosahedral and decagonal phases, have been found to exhibit a coherent orientational relationship during their growth and/or transformation processes.[11,12] The coherent orientational relationship has also been found between icosahedral quasicrystalline and crystalline phases.[13,14] These orientational relationships have indicated a close structural linkage between different quasicrystalline and corresponding crystalline structures. For example, it has been pointed out that a common structural subunit, e. g., MacKay icosahedra (MI), maintains parallelism of its orientation across the quasicrystalline and crystalline phase boundaries.[13] This parallelism of MacKay icosahedra has also been found to exist in the polycrystalline aggregates of a rapidly solidified Al–Mn–Fe–Si alloy.[14] The aforesaid interrelationships have demonstrated an orientational relationship between quasicrystalline-quasicrystalline and quasicrystalline-crystalline phases, etc.; however, a specific interrelationship has been observed in specific alloy systems only.[11–14]

The present communication deals with the detailed TEM investigation of the occurrence of quasicrystalline and related crystalline phases in a rapidly solidified $Al_{78}Mn_{20}Ge_2$ alloy. It may be pointed out that this alloy system with higher Ge concentration (>2 at. %) has been investigated by Schaefer and Bendersky[12] and Mukhopadhyay *et al.*[15] in regard to the occurrence of icosahedral and decagonal phases. The rapidly solidified alloy $Al_{78}Mn_{20}Ge_2$ investigated in the present work is unique in the sense that it exhibits the simultaneous occurrence of almost all the quasicrystalline and related phases reported so far. Another remarkable observation found in this investigation is that the orientational invariance of the icosahedral motif occurs across the phase boundaries of all these phases. In the present study it has been shown that the irrational twin variants can also be related by noncrystallographic (irrational) mirror planes of the type $(\tau, \tau^2, 1)$. Based on this relation simulation of the observed EDP's from the twin variants has been carried out. Diffraction evidences showing the route of the icosahedral-to-crystalline transformation is also presented.

## II. EXPERIMENTAL

Pure (99.99%) constituent metals Al, Mn, and Ge were taken in the atomic ratio of $Al_{78}Mn_{20}Ge_2$ and were melted by R. F. heating under argon atmosphere in a silica tube. The ingot was then subjected to melt-spinning (copper wheel of 13.7 cm diameter, 3500 rpm). The ribbons formed were of 1 to 2 mm width and 30 to 40 $\mu$m thickness. The ribbons were then electropolished (80% ethanol + 20% perchloric acid) and subjected to electron microscopic investigation at 100 KV (Philips-CM-12).

## III. RESULTS AND DISCUSSION

The icosahedral quasicrystal and related phases have usually been observed in diverse alloy systems.[2–9] However, during the electron microscopic characterization of the present alloy it has been found that almost all types of quasicrystalline phases related with icosahedral point-group (e.g., primitive and face-centered icosahedral, decagonal, and rational approximant structures) are simultaneously present in this system. Together with these phases a new cubic crystalline phase has also been observed. The selected area diffraction (SAD) study of the various local areas reveals that all the phases bear a well-defined orientational relation amongst themselves. The cubic phase has been found to show an unusual type of twin relation within itself. The occurrence of various quasicrystalline and crystalline phases and their coherent orientational relationship are described in the next section.

## A. Simple and face-centered icosahedral phases

Figures 1(a) and 1(b) show the 2-fold zone axis patterns from primitive and face-centered icosahedral phases, respectively. Pattern (a) contains both types of spots (spots along 5-fold directions scaling by both $\tau$ and $\tau^3$) whereas pattern (b) contains spots scaling only by $\tau$, indicating the nonprimitive type of reciprocal lattice (Ebalard, 1989). The superlattice spots occurring along the 5-fold direction due to the nonprimitive type of lattice are indicated by arrows. The indexing of this pattern [Fig. 1(b)] has been accomplished and it has been found that all the spots have either all even or all odd indices. Figures 1(c) and 1(d) show 5-fold and 3-fold patterns, respectively, from the face-centered icosahedral (FCI) phase. It should be pointed out that the FCI phase has been observed mostly in the alloy system $Al_{65}Cu_{20}M_{15}$ (M = Cr, Mn, Fe, Ru, and Os).[6] The only alloy known so far that exhibits the FCI phase and does not contain copper is $Al_{70}Pd_{15}Mn_{15}$.[16] The rapidly solidified $Al_{78}Mn_{20}Ge_2$ alloy represents yet another alloy system in this category.

## B. The crystalline phase and irrational twinning

Figures 2(a), 2(b), and 2(c) show the [001], [111], and [11$\bar{1}$], respectively, zone axis diffraction patterns of

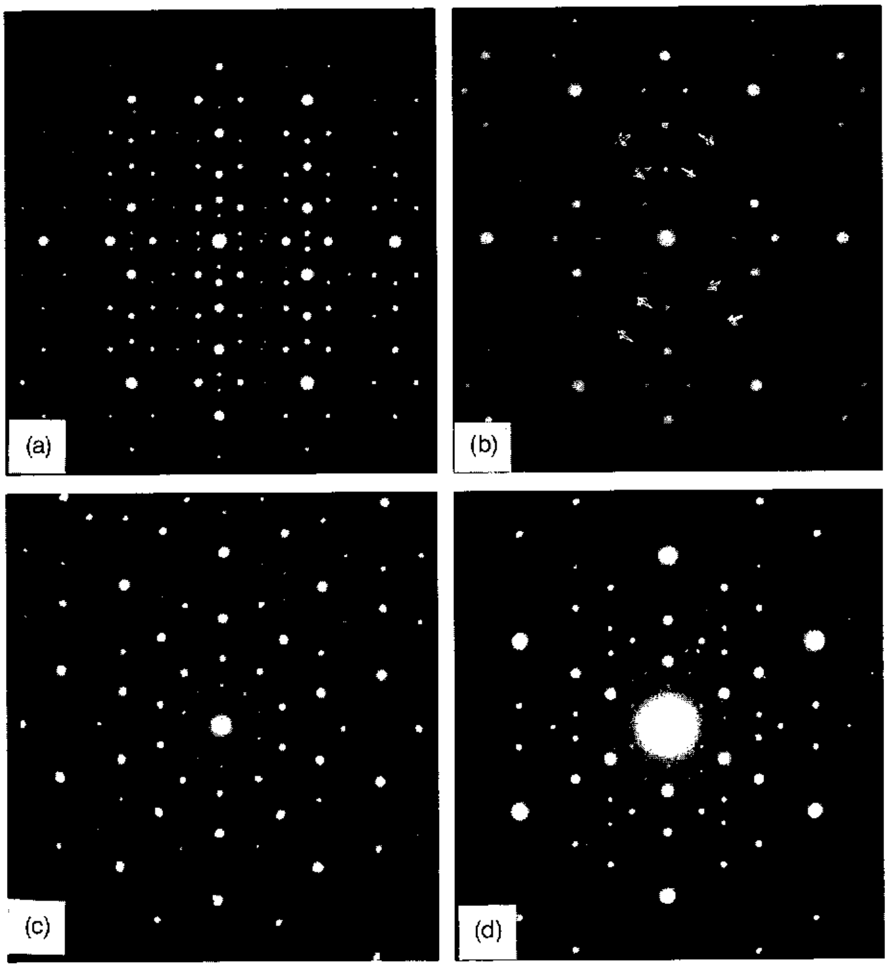


FIG. 1. Selected area diffraction (SAD) patterns showing the presence of both primitive and face-centered icosahedral phase (FCI) in Al–Mn–Ge: (a) Twofold SAD pattern from primitive I-phase. (b–d) SAD patterns, respectively, along 2-fold, 5-fold, and 3-fold zone axes from FCI phase.

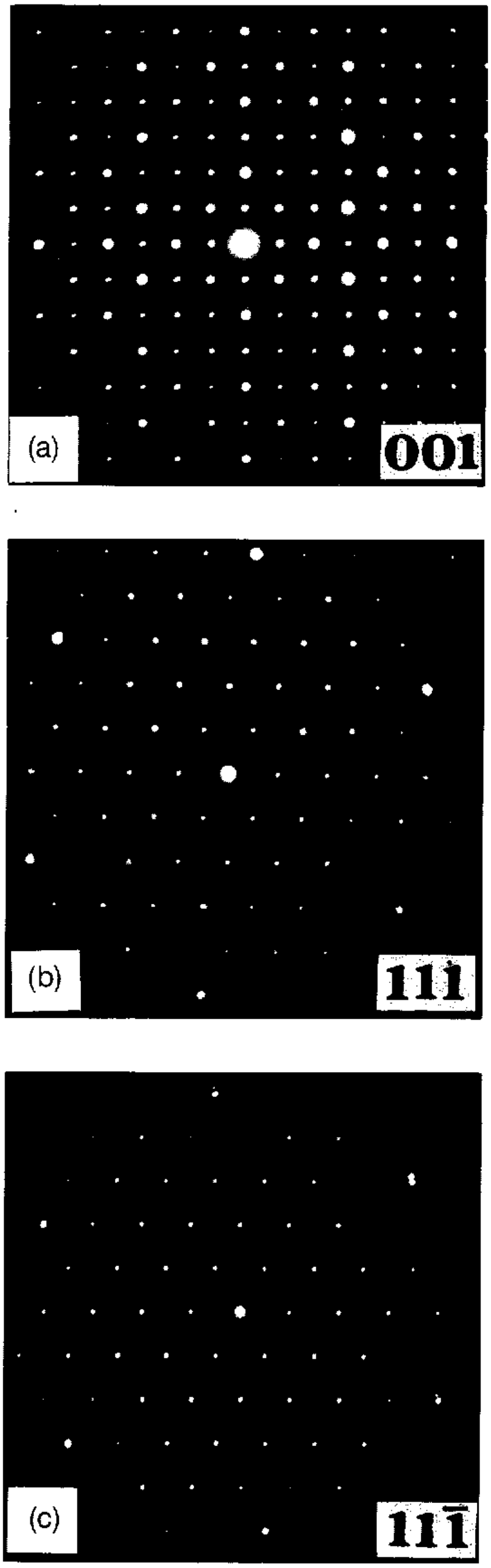


FIG. 2. SAD patterns from cubic crystalline phase of Al–Mn–Ge showing (a) [001], (b) [111], and (c) [11$\bar{1}$] sections of the corresponding reciprocal lattice.

the cubic phase with lattice parameter 12.6 Å. Keeping in view the similarity of the observed EDP's, its crystal structure can be assigned as the crystal structure of $\alpha$–Al–Mn–Si.[17] The Al–Mn–Ge equilibrium phase diagram features only one phase having the $Cu_2Sb$ type crystal structure with space group $P^4/nmm$.[18] Thus the crystalline phase observed in the present investigation (Fig. 2) is a new phase that is isostructural to $\alpha$–Al–Mn–Si.

Figures 3(a), 3(b), and 3(c) show the SAD patterns obtained from the Al–Mn–Ge phase exhibiting 5-fold, 2-fold, and 3-fold symmetries, respectively. These patterns bear strong resemblance to the composite twin patterns reported for $\alpha$–Al–Mn–Si by Koskenmaki *et al.* (1986)[13] and for bcc Al–Mn–Fe–Si by Bendersky *et al.* (1989).[14] The latter authors have shown that these types of patterns arise due to an unusual type of twinning among cubic variants. The lattices of the different cubic variants are related to each other by 72° rotation about a $[\tau, 1, 0]$ type of irrational axis and hence this type of twinning may be called irrational twinning. This is unusual in the sense that they do not possess coincidence site lattices (CSL).[14] Here, these variants have one common feature, the presence of icosahedral motifs (MacKay-Icosahedra, MI) in their structures. In this type of twinning the lattices are flipping from one crystal to another in such a way that the orientation of the icosahedral motif remains invariant. This can be represented diagrammatically as in Fig. 4 for a two-dimensional square lattice having a pentagonal motif. The orientational invariance of a pentagonal motif can be seen in this noncoincidence site lattice type of twinning of 2D square crystal. Simulation of the EDP's showing the icosahedral point group has been done by Bendersky *et al.* (1989),[14] taking into consideration the bcc (lattice points only) structure. However, it may be pointed out that these twin variants can also be related by irrational mirror planes of the type $(1, \tau, \tau^2)$. Such type of mirror operation will leave the orientation of the icosahedral motif (MI) unchanged across the grain boundaries. Since the orientation of the icosahedral motif is invariant across the grain boundaries, the orientation of the lattice corresponding to different variants will depend only on the position of glue atoms. This mirror relation directly elucidates the required changes in the glue atoms. On the basis of this mirror relation it can also be discerned that these irrational twins will be low energy configurations only when at the interface the two structures share the same icosahedral motif, since this configuration will have either zero or minimum strain at the twin boundary.

The generation of the different variants can be given as follows:

$$V_2 = V_1 M(1)$$

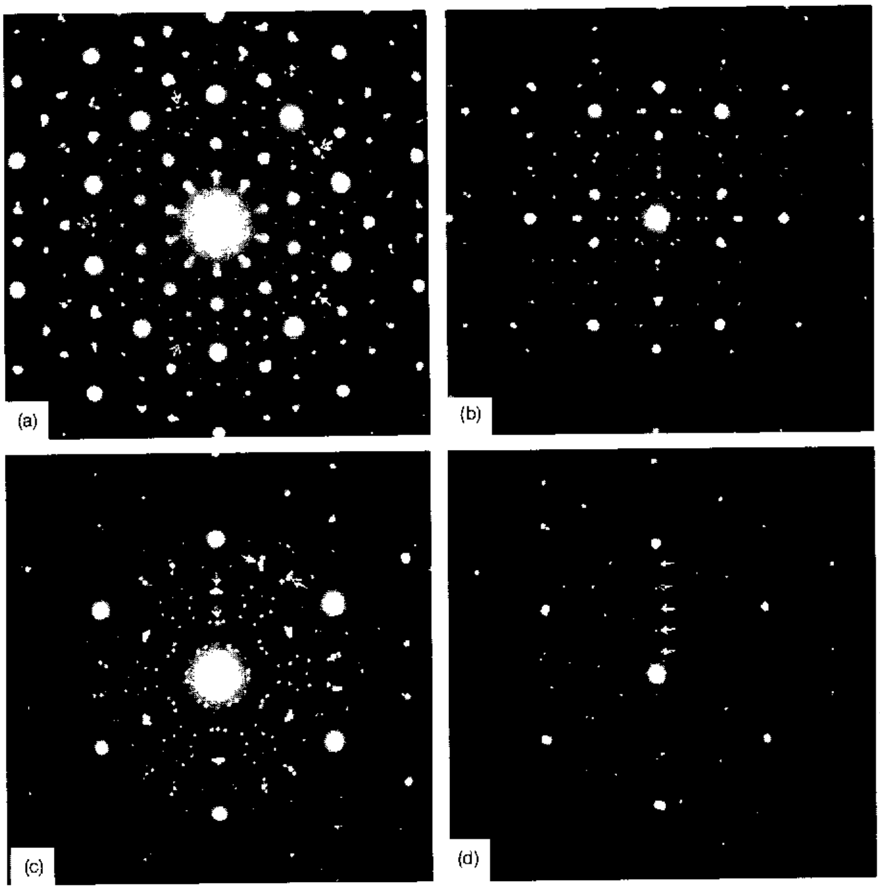


FIG. 3. Composite electron diffraction patterns (EDP's) from irrational twin variants and I-phase grains along equivalent (a) 5-fold zone axis [(350) spots indicated by arrows from five different irrational twin variants confirm the presence of [530] orientation]. (b) Twofold zone axis and (c) 3-fold zone axis containing only two variants of $\langle 111 \rangle$ type of orientations; spots indicated by arrows are from I-phase. (d) shows [13, 5, 0] orientation (spots indicated by arrows) together with [111] orientation.

$$V_3 = V_2 M(2)$$
$$V_4 = V_1 M(3)$$
$$V_5 = V_4 M(4)$$

Here $V_1$, $V_2$.... and $V_5$ are the zone axes of the first, second.... and fifth variants, respectively, and $M_1$, $M_2$, $M_3$, and $M_4$ are the matrices corresponding to the mirror relation across the planes $(1, \tau, \bar{\tau}^2)$, $(\tau, \tau^2, 1)$, $(1, \tau, \tau^2)$, and $(\tau, \tau^2, \bar{1})$, respectively.

$$M(1) = \frac{1}{2}\begin{bmatrix} \tau & -\tau^{-1} & 1 \\ -\tau^{-1} & 1 & \tau \\ 1 & \tau & -\tau^{-1} \end{bmatrix}$$

$$M(2) = \frac{1}{2}\begin{bmatrix} 1 & -\tau & -\tau^{-1} \\ -\tau & -\tau^{-1} & -1 \\ -\tau^{-1} & -1 & \tau \end{bmatrix}$$

$$M(3) = \frac{1}{2}\begin{bmatrix} \tau & -\tau^{-1} & -1 \\ -\tau^{-1} & 1 & -\tau \\ -1 & -\tau & -\tau^{-1} \end{bmatrix}$$

$$M(4) = \frac{1}{2}\begin{bmatrix} 1 & -\tau & \tau^{-1} \\ -\tau & -\tau^{-1} & 1 \\ \tau^{-1} & 1 & \tau \end{bmatrix}$$

The variants related through 5-fold rotation about $[\tau, 1, 0]$ can also be generated by the operation of the following rotation matrix *M(R)*:

$$M(R) = \frac{1}{2}\begin{bmatrix} \tau & \tau^{-1} & 1 \\ \tau^{-1} & 1 & -\tau \\ -1 & \tau & \tau^{-1} \end{bmatrix}$$

The zone axes of the five cubic variants responsible for the generation of icosahedral-point-group can be obtained either by mirror relation or rotation relation using the above matrices and are listed in Table I. Using the mirror and rotation relations, based on the crystal structures of $\alpha$–Al–Mn–Si (*Pm*3), EDP has been simulated. Figures 5(a), 5(b), and 5(c) present the simulated EDP's corresponding to 5-fold, 2-fold, and 3-fold of irrational twin. For the simulation of the 5-fold, 2-fold, and 3-fold EDP's, $\langle 530 \rangle$, $\langle 100 \rangle$, and $\langle 111 \rangle$ directions have been chosen, respectively, for

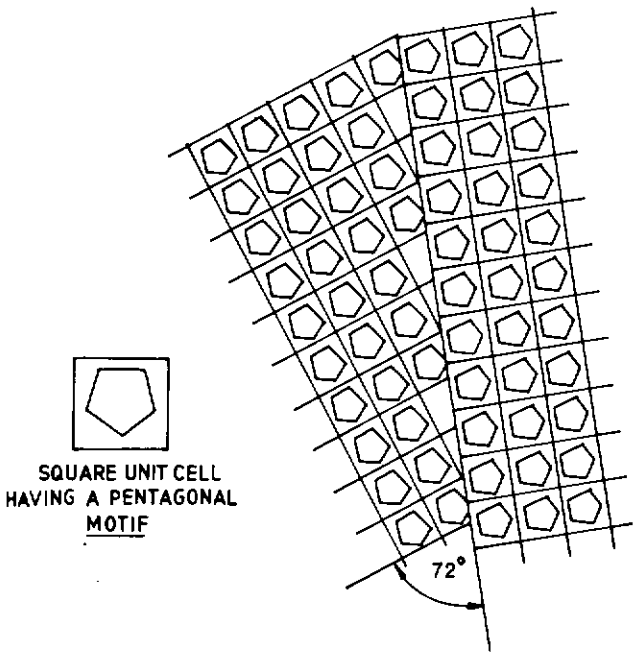


FIG. 4. Schematic representation of (two-dimensional) irrational twin of two square lattices having pentagonal motifs. The presence of non-coincident lattice sites at the boundary can be seen. The orientational invariance of pentagonal motifs across the grain boundary can also be noticed.

the matrix operation. Comparison of the experimentally observed and corresponding simulated patterns shows that Figs. 3(a) and 3(b) are the true representatives of five irrationally twinned cubic variants. Figure 3(c) contains only two variants of the $\langle 111 \rangle$ type, and the remaining three of the $\langle 13, 5, 0 \rangle$ type of orientations are absent. The additional spots in the experimental patterns are due to the I-phase. Presence of the $\langle 13, 5, 0 \rangle$

TABLE I. Relation among zone axes of five crystalline variants producing icosahedral symmetry.

| | Zone axes | | |
|---|---|---|---|
| Variants | 5-fold | 3-fold | 2-fold |
| Variants related by mirrors | | | |
| 1st | $5,\bar{3},0$ | $1,1,1$ | $1,0,0$ |
| 2nd | $5,\bar{3},0$ | $1,1,1$ | $8,\bar{3},5$ |
| 3rd | $5,\bar{3},0$ | $\bar{5},\overline{13},0$ | $5,\bar{8},3$ |
| 4th | $5,\bar{3},0$ | $0,\bar{5},\overline{13}$ | $8,\bar{3},\bar{5}$ |
| 5th | $5,\bar{3},0$ | $0,\bar{5},\overline{13}$ | $5,\bar{8},\bar{3}$ |
| Variants related by rotation | | | |
| 1st | $5,3,0$ | $1,1,1$ | $1,0,0$ |
| 2nd | $5,3,0$ | $13,0,5$ | $8,3,\bar{5}$ |
| 3rd | $5,3,0$ | $13,0,\bar{5}$ | $5,8,\bar{3}$ |
| 4th | $5,3,0$ | $1,1,\bar{1}$ | $5,8,3$ |
| 5th | $5,3,0$ | $5,13,0$ | $8,3,5$ |

type of orientation of primitive cubic variants is evident from the SAD shown in Fig. 3(d). The high resolution electron micrographs taken from the region exhibiting 2-fold [Fig. 3(b)] and 3-fold [Fig. 3(c)] SAD patterns due to irrational twinning are shown in Figs. 6(a) and 6(b), respectively. Figure 6(a) depicts the high resolution fringes corresponding to $\{100\}$ planes, confirming the crystalline nature of the region. In Fig. 6(b) the $\langle 111 \rangle$ and $\langle 13, 5, 0 \rangle$ types of variants (indicated by arrows) are also quite evident.

In passing, it may be mentioned that in addition to the diffraction spots due to twin variants, the spots due to the icosahedral phase are invariably present in Fig. 3. This is in accordance with the earlier observations[19,20] that the crystalline variants are formed due to the crystallization of the icosahedral phase. Consequently an orientational relationship among all the crystalline variants and icosahedral phase would result.

### C. Orientation relation among icosahedral, decagonal, and crystalline phases

In the above discussion we have seen that the orientation of motifs remains invariant across the boundaries of the irrational twin variants of a cubic phase. This feature shows its presence in a more general way in this alloy. Figure 7 shows a superposition of icosahedral 2-fold and a decagonal 2-fold. It can be noticed that the 5-fold direction of the i-phase is parallel to the 10-fold direction of the decagonal phase, representing the same invariance of MacKay-Icosahedra that is the basic unit for these quasicrystalline structures. This is a case of icosahedral-to-decagonal transformation. Such type of orientation relation has already been reported.[11,12] Figures 8(a) and 8(b) show the SAD pattern and high resolution micrograph from a region where the crystalline cubic phase and decagonal phase both are co-existing, have a well-defined orientation relation. Even though the cubic-twin does not form directly from the decagonal phase, it exhibits an orientation relationship because it is derived from the same parent icosahedral phase. In Fig. 9(a) the [001] is parallel to the F type 2-fold of the decagonal phase and the line parallel to the 10-fold direction passes through the (530) reflection, showing that the 10-fold of decagonal is parallel to the [530] direction of the cubic phase. Here once again the orientational invariance of the icosahedral motif is maintained.

### D. Rational approximants

While the ideal quasicrystal is expected to exhibit strict icosahedral symmetry, observed patterns from many alloys show deviations. These have been ascribed to phason defects or analyzed on the basis of rational

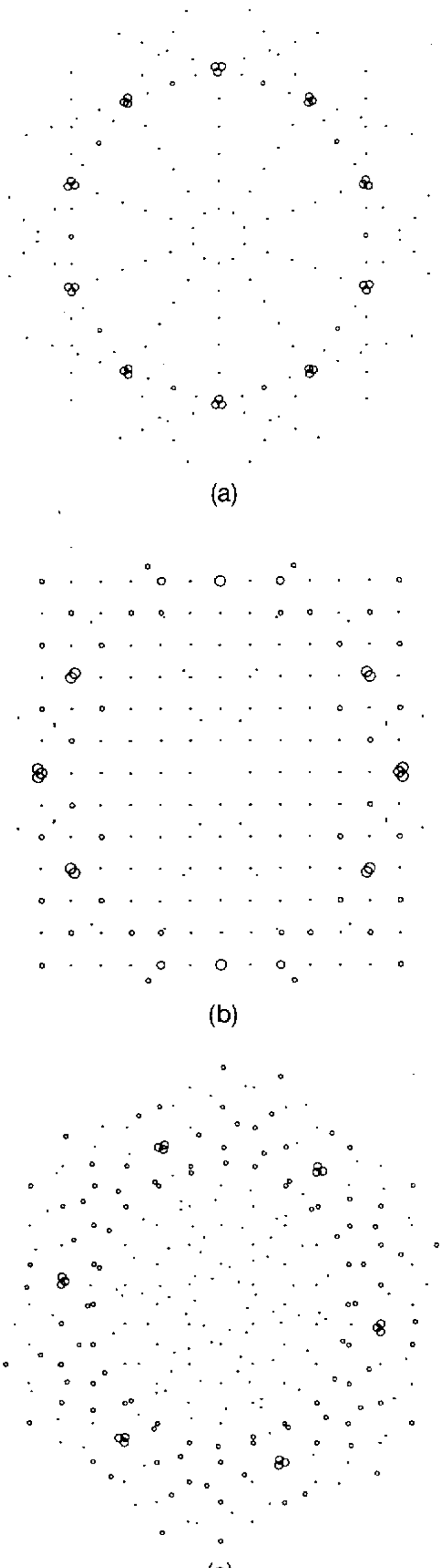


FIG. 5. Simulated EDP's of mirror related five irrational cubic twins ($\alpha$–Al–Mn–Ge) showing icosahedral point group. (a–c) are along equivalent 5-fold, 2-fold, and 3-fold zones.

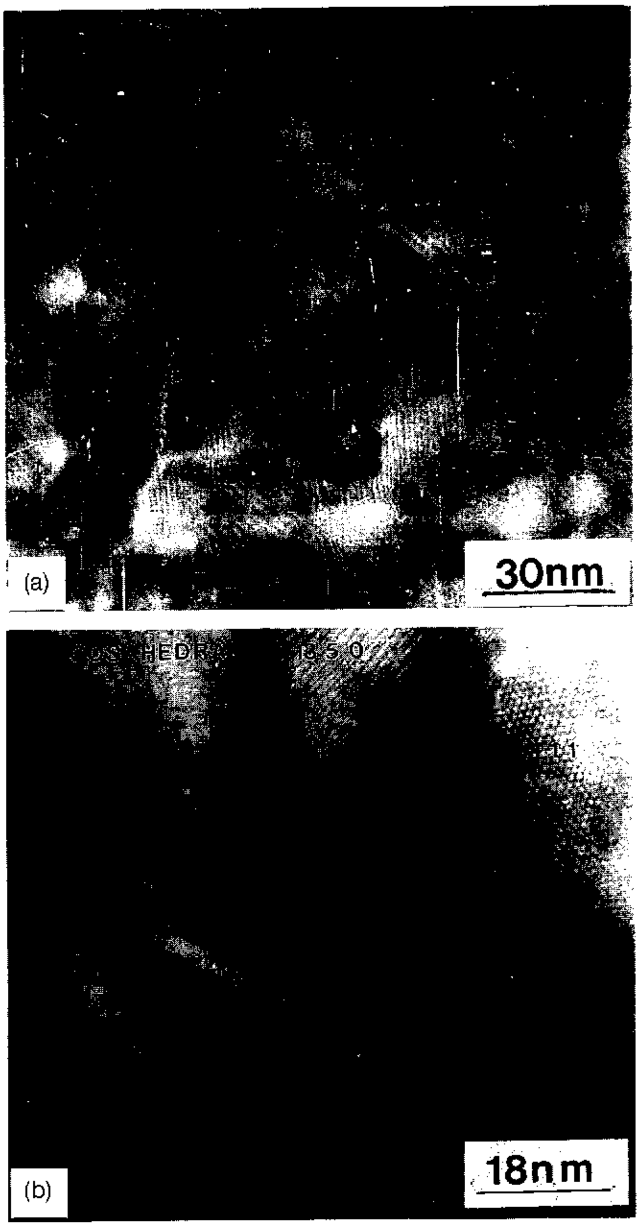


FIG. 6. High resolution micrographs of irrational cubic twins in the equivalent (a) 2-fold orientation and (b) 3-fold orientation. Variants in [111] and [13, 5, 0] orientation are indicated.

approximants (RA).[21] Figures 9(a), 9(b), and 9(c) show the SAD from rational approximant structures in the Al–Mn–Ge system.

## IV. SUMMARY

Thus from the above discussions we see that in the rapidly solidified $Al_{78}Mn_{20}Ge_2$ system almost all the quasicrystalline related phases grow during rapid solidification having a unique orientational relationship among themselves. The basic building block of all these phases, the icosahedral motif, remains invariant across

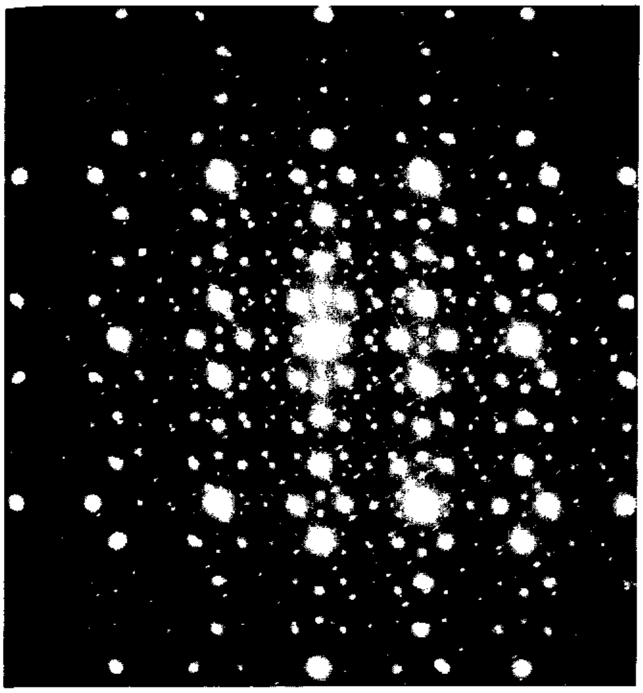

FIG. 7. Composite electron diffraction patterns from icosahedral and decagonal phases. The 5-fold direction of the I-phase is parallel to the 10-fold direction of the decagonal phase.

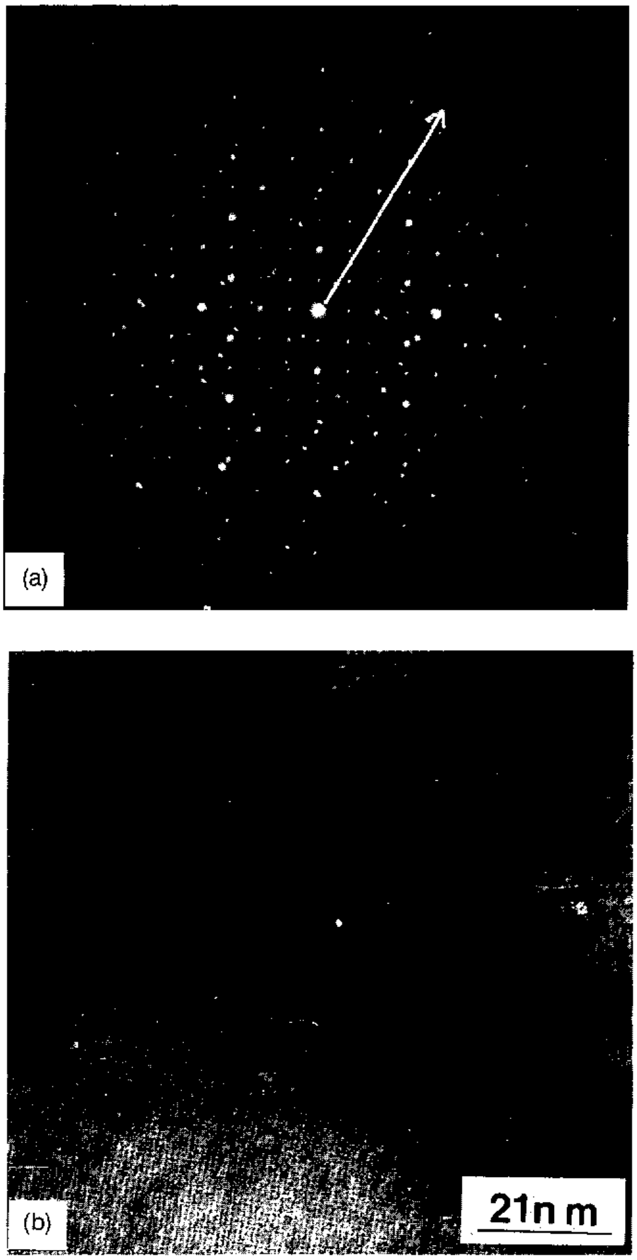


FIG. 8. (a) Superposed pattern due to cubic phase (001 section) and decagonal phase (F type 2-fold). The 10-fold axis of the decagonal phase is passing through the (530) type of reflection. (b) High resolution micrograph from the same region, showing the cubic and decagonal variants.

their grain boundaries. Keeping in view the group-subgroup relation,[22] it appears that the primitive icosahedral phase forms in the melt and subsequently undergoes transformation to the other phases, such that the orientation of the motif remains invariant. The present results clearly show the structural interrelation among the various known quasicrystalline and crystalline phases. The simulation studies of EDP's corresponding to irrational twin-variants reveal that the structures of different crystalline variants are related by mirrors of $(1, \tau, \tau^2)$ type planes. It may be pointed out that although various studies in different alloy systems indicate a close relation between quasicrystalline and crystalline phases, this feature has been manifested in a more general manner by $Al_{78}Mn_{20}Ge_2$. These observations are of considerable importance from the viewpoint of the study of detailed atomic structures of quasicrystalline phases, especially in structural modeling.

## ACKNOWLEDGMENTS

The authors are grateful to Professor A. L. MacKay (Birkbeck College, London) for the initial encouragement. Helpful discussions with Professor L. A. Bendersky (Centre of Materials Research, The Johns Hopkins University), Professor S. Lele, and Dr. R. K. Mandal (Department of Metallurgical Engineering, Banaras Hindu University) are also acknowledged. The present work was carried out under a research project sponsored by the Department of Non-Conventional Energy Sources.

## REFERENCES

1. D. Shechtmann, I. Blech, D. Gratias, and J. W. Cahn, Phys. Rev. Lett. **53**, 1951 (1984).
2. S. J. Poon, A. J. Drehman, and K. R. Lawless, Phys. Rev. Lett. **55**, 2324 (1985).
3. H. S. Chen and A. Inoue, Scripta Metall. **21**, 527 (1987).

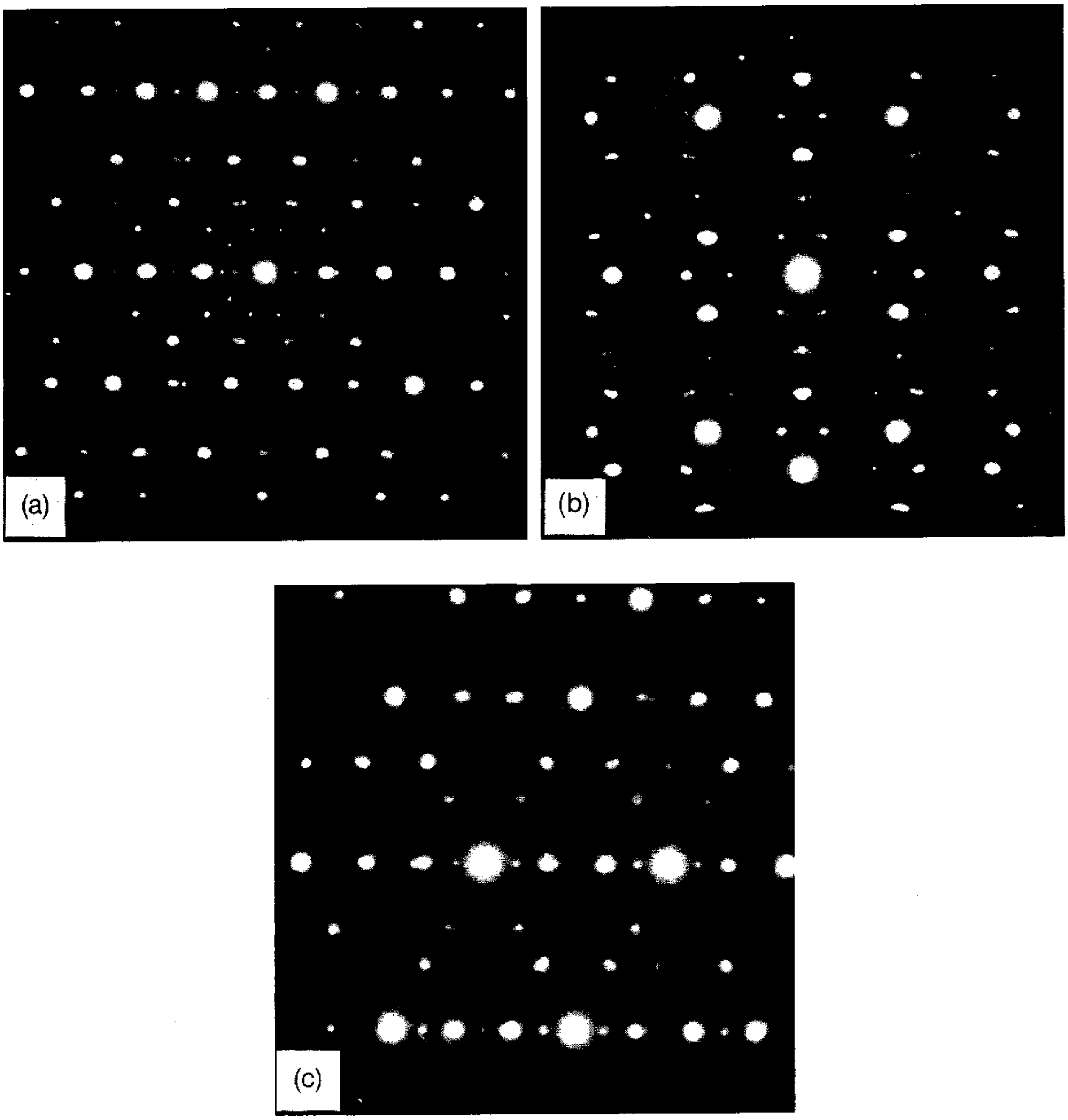

FIG. 9. SAD patterns from a rational approximant structure of the I-phase along (a) 5-fold, (b) 2-fold, and (c) 3-fold zone axes.


4. L. A. Bendersky, Phys. Rev. Lett. **55**, 1461 (1985).
5. K. Chattopadhyay, S. Lele, N. Thangaraj, and S. Ranganathan, Acta Metall. **35**, 727 (1987).
6. A. P. Tsai, A. Inoue, and T. Masumoto, Jpn. J. Appl. Phys. **26**, L1505 (1987).
7. S. Ebalard and F. Spaepen, J. Mater. Res. **4**, 39 (1989).
8. K. Chattopadhyay and N. K. Mukhopadhyay, Mater. Sci. Forum **22–24**, 639 (1987).
9. C. H. Chen and H. S. Chen, Phys. Rev. B **33**, 2814 (1986).
10. D. S. Rokhsar, N. D. Mermin, and D. C. Wright, Phys. Rev. B **35**, 5487 (1987).
11. N. P. Lalla, R. S. Tiwari, and O. N. Srivastava, Philos. Mag. B **63**, 629 (1991).
12. R. J. Schaefer and L. A. Bendersky, Scripta Metall. **20**, 745 (1986).
13. D. C. Koskenmaki, H. S. Chen, and K. V. Rao, Phys. Rev. B **33**, 5326 (1986).
14. L. A. Bendersky, J. W. Cahn, and D. Gratias, Philos. Mag. B **60**, 837 (1989).
15. N. K. Mukhopadhyay, G. N. Subbanna, K. Chattopadhyay, and S. Ranganathan, Proc. IV Asia-Pacific Conference on Electron Microscopy, Bangkok, 187 (1988).

16. A. P. Tsai, A. Inoue, Y. Yokoyama, and T. Masumoto, Philos. Mag. Lett. **61**, 9 (1990).
17. M. Cooper and K. Robinson, Acta Cryst. **20**, 614 (1966).
18. P. Villars and L. D. Calvert, *Pearson's Handbook of Crystallographic Data for Intermetallic Phases* (American Society for Metals, Metal Park, OH, 1985).
19. F. H. Li, G. Z. Pan, S. Z. Tao, M. J. Hui, Z. H. Mai, X. S. Chen, and L. Y. Cai, Philos. Mag. B **59**, 535 (1989).
20. K. K. Fung and Y. Q. Zhow, Philos. Mag. B **54**, L27 (1986).
21. N. K. Mukhopadhya, K. N. Ishihara, S. Ranganathan, and K. Chattopadhyay, Acta Metall. (submitted, 1990).
22. J. Devaud-Rzepski, A. Quivy, Y. Calvayrae, M. Cornier-Quiquandon, and D. Gratias, Philos. Mag. B **60**, 855 (1989).